

THERMAL DECOMPOSITION OF AQUEOUS MANGANESE NITRATE SOLUTIONS AND ANHYDROUS MANGANESE NITRATE. PART 4. NON-ISOTHERMAL KINETICS

T.J.W. DE BRUIJN, A.N. IPEKOĞLU, W.A. DE JONG and P.J. VAN DEN BERG

Delft University of Technology, Julianalaan 136, 2628 BL Delft (The Netherlands)

(Received 22 October 1980)

ABSTRACT

Kinetic parameters for the decomposition of aqueous manganese nitrate solutions were derived from non-isothermal experiments in air. First, most of the water evaporates to a solution containing approximately equimolar quantities of water and manganese nitrate which then decomposes in two steps to MnO_2 . The first step can be described by a model valid for two-dimensional growth of a constant number of nuclei, viz. $g(\alpha) = [-\ln(1 - \alpha)]^{1/2}$, and the second by a model based on a surface reaction, viz. $g(\alpha) = 1 - (1 - \alpha)^{1/3}$.

The decomposition of anhydrous manganese nitrate most probably occurs via nuclei formation with a decreasing rate and one-dimensional growth of the nuclei formed. The model $g(\alpha) = [-\ln(1 - \alpha)]^{0.6}$ described the measurements satisfactorily. The parameters in the above models closely agree with results from isothermal experiments.

INTRODUCTION

The thermal decomposition of aqueous manganese nitrate solutions is being studied to investigate its potential value as a method of producing battery-grade MnO_2 . Part 1 of this series [1] was concerned with the mechanism of the decomposition. It was shown that first, most of the water evaporates to a concentrated solution with a composition of about 1 mole H_2O per mole $\text{Mn}(\text{NO}_3)_2$, which then decomposes in two steps to $\gamma\text{-MnO}_2$. The two chemical steps are referred to as first and second decomposition step, respectively. In the first decomposition step the residual water evolves and only part of the $\text{Mn}(\text{NO}_3)_2$ decomposes into MnO_2 and almost exclusively NO_2 (N_2O_4). In the second step the remainder of the $\text{Mn}(\text{NO}_3)_2$ decomposes. The first decomposition step is caused and accelerated by water vapour; without water (anhydrous manganese nitrate) only one decomposition step occurs.

In Part 2 [2] the heat of reaction was measured for the above decomposition reactions and in Part 3 [3] the kinetics were established from isothermal experiments. The first decomposition step could be described best by the model $[-\ln(1 - \alpha)]^{1/2} = 8.9 \times 10^{11} \exp(-121000/RT)t$. For the second step and the decomposition of anhydrous manganese nitrate several models fitted

TABLE 1

Kinetic parameters for the second decomposition step and decomposition of anhydrous manganese nitrate from isothermal experiments [3] (A = pre-exponential factor, E = activation energy)

Model	Second decomposition step		Decomposition of anhydrous manganese nitrate	
	A (s^{-1})	E ($kJ\ mole^{-1}$)	A (s^{-1})	E ($kJ\ mole^{-1}$)
$-\ln(1 - \alpha)$	6.5×10^{12}	143	2.6×10^7	93
$[-\ln(1 - \alpha)]^{2/3}$	2.0×10^{12}	139	1.4×10^7	90
$1 - (1 - \alpha)^{1/2}$	8.6×10^{11}	140		
$1 - (1 - \alpha)^{1/3}$	1.6×10^{12}	143	1.1×10^7	94

the data equally well and no selection could be made from them. The kinetic parameters extracted from the various models were fairly similar and are given in Table 1. To make a selection from the various models and to obtain more information about the actual mechanism of the decomposition, non-isothermal experiments were performed, the results of which are described here.

EXPERIMENTAL

Equipment

The experiments were performed in a Stanton-Redcroft TG 750 thermo-balance through which $100\ ml\ min^{-1}$ air, dried over molecular sieves, was passed. The sample weights were in the range 2–4 mg.

Material

A reagent-grade aqueous manganese nitrate solution containing 59.9 wt.% $Mn(NO_3)_2$, 2.7 wt.% HNO_3 and 37.4 wt.% H_2O was obtained from J.T. Baker Chemicals Corp.

Procedures

The procedure for the experiments on the decomposition of the solution was as follows. First, most of the water and all nitric acid [4] was evaporated by heating the solution to 110 – $120^\circ C$ at a rate of $15^\circ C\ min^{-1}$. A virtually constant weight was invariably obtained which corresponded to a composition of approximately 1 mole of H_2O per mole of $Mn(NO_3)_2$ [1]. The sample was then heated at a constant rate until the decomposition was complete.

Anhydrous manganese nitrate was prepared from the same solution. After removal of most of the water by heating the solution to $\approx 100^\circ C$, vacuum

(≈ 3 kPa) was applied for 1 h to remove the remainder of the water. The pressure was then raised to atmospheric, the air flow adjusted to 100 ml min^{-1} , and the sample heated at a constant rate until the reaction was complete.

Heating rates were varied between ~ 1.6 and $\sim 11^\circ\text{C min}^{-1}$ for all decompositions. Time (i.e. temperature)—conversion curves were calculated by taking the weight loss observed for each decomposition step to correspond to 100% conversion.

MODELLING

The general equation used most often to describe non-isothermal reactions is

$$\int \frac{d\alpha}{f(\alpha)} = g(\alpha) = \int k dt \quad (1)$$

where α = conversion, k = reaction rate constant (s^{-1}), t = time(s), and $f(\alpha)$ = a function of the conversion, its form depending on the mechanism of the reaction.

Generally, the same equations for $g(\alpha)$ may be used as are valid for isothermal reactions. For example, for homogeneous reactions we have

$$f(\alpha) = \frac{1}{1-p} (1-\alpha)^p \quad p \neq 1 \quad (2)$$

where p is the order of the reaction. Integration results in

$$g(\alpha) = 1 - (1-\alpha)^{1-p} = \int k dt \quad p \neq 1 \quad (3)$$

where $g(\alpha)$ is identical to the expression valid for isothermal reactions.

For $p = 1/2$ and $p = 2/3$, eqn. (3) is identical to equations valid for surface reactions with cylindrical and spherical geometry, respectively. Very often eqn. (1) is also used for nuclei growth type (Avrami—Erofeev type) reactions, which for isothermal reactions can be represented by

$$[-\ln(1-\alpha)]^{1/n} = kt \quad \text{with } n = 1, 2, 3 \text{ and } 4 \quad (4)$$

For non-isothermal reactions eqn. (4) is often differentiated to obtain $f(\alpha)$

$$f(\alpha) = n(1-\alpha)[- \ln(1-\alpha)]^{1-1/n} \quad (5)$$

In fact this expression is only valid for isothermal reactions. However, $f(\alpha)$ is often substituted in eqn. (1) to give an expression which is used to describe non-isothermal reactions (e.g. refs. 5 and 6). This is not a correct procedure, as has been pointed out by Henderson [7]; strictly speaking, eqn. (5) may only be used for isothermal transformations. Fortunately, the error which is made by still using it is negligible or small for the most frequently occurring types of reaction [8]. For reactions with a constant number of growing nuclei it was derived that eqn. (1), after substitution of eqn. (5), results in correct kinetic parameters. The correct overall activation energy is also obtained for a reaction with growing nuclei and new nuclei formation at a con-

stant rate. Only the pre-exponential factor (A) can be slightly off, the error depending on the difference in the activation energies for growth and nucleation [8]. In view of the above, eqn. (1) combined with eqn. (5) for $f(\alpha)$ was applied to analyse the results obtained in the present work. For the integral on the left-hand side of eqn. (1) the normal $g(\alpha)$ functions result which are generally used to analyse isothermal experiments. The integral on the right-hand side of eqn. (1) is solved according to Doyle's method [9], which results in

$$\int k dt = \int A \exp(-E/RT) dt = \frac{AE}{\beta R} p(x) \quad (6)$$

in which

$$p(x) = \int_x^\infty \frac{\exp(-x)}{x^2} dx \quad (7)$$

where $x = E/RT$, R = gas constant ($\text{J mole}^{-1} \text{K}^{-1}$), A = pre-exponential factor (s^{-1}), T = temperature (K), E = activation energy (J mole^{-1}), and β = heating rate (K s^{-1}). The function $p(x)$ has been approximated by several investigators. The most widely used approximation is that of Coats and Redfern [10], who applied the relation

$$\int_x^\infty e^{-x} x^{-b} dx \approx x^{1-b} e^{-x} \sum_{m=0}^{\infty} \frac{(-1)^m (b)^m}{x^{m+1}} \quad (8)$$

Using the first two terms, this results in

$$g(\alpha) = \int k dt = \frac{AR}{\beta E} T^2 \exp\left(-\frac{E}{RT}\right) \left(1 - \frac{2RT}{E}\right) \quad (9)$$

Several $g(\alpha)$ functions were tested with this general expression to describe the measured temperature-conversion curves. The models for $g(\alpha)$ which were tested are given in Table 2. These are the models which gave the best fit for the isothermally obtained time-conversion curves [3]. Only for the decomposition of anhydrous manganese nitrate were some additional nuclei

TABLE 2

Kinetic models tested

Model	Type	Reaction
$[-\ln(1-\alpha)]^{1/n}$ $1/n = 1/4, 1/3, 1/2$	Nuclei growth (Avrami-Erofeev)	1
$-\ln(1-\alpha)$	First order	2, 3
$[-\ln(1-\alpha)]^{2/3}$	Nuclei growth	2, 3
$1 - (1-\alpha)^{1/3}$	Surface reaction (spherical geometry)	2, 3
$[-\ln(1-\alpha)]^{1/n}$ $1/n = 0.6, 0.7, 0.8$	Nuclei growth	3

1 = First decomposition step.

2 = Second decomposition step.

3 = Decomposition of anhydrous manganese nitrate.

growth type models tested with $n = 0.6, 0.7$ and 0.8 .

To obtain the kinetic parameters, use was made of a standard computer programme varying A and E until the minimum was obtained of

$$\sum_{i=1}^m \left[\frac{g(\alpha)_{\text{theor}} - g(\alpha)_{\text{exp}}}{g(\alpha)_{\text{exp}}} \right]^2 \quad (10)$$

in which

$$g(\alpha)_{\text{theor}} = \frac{AR}{\beta E} T^2 \exp\left(-\frac{E}{RT}\right) \left[1 - \frac{2RT}{E}\right] \quad (11)$$

$$g(\alpha)_{\text{exp}} = \text{the model which is tested, e.g. } [-\ln(1 - \alpha)]^{1/n} \quad (12)$$

m = number of pairs of temperature and conversion for which eqns. (11) and (12) are calculated. To discriminate between different models, the variance was calculated which is defined as

$$v = \sum_{i=1}^m \left(\frac{\alpha_{\text{theor}} - \alpha_{\text{exp}}}{m - 2} \right)^2$$

α_{theor} was calculated from $g(\alpha)_{\text{theor}}$ [eqn. (11)] and α_{exp} represents the measured conversion.

RESULTS AND DISCUSSION

The measured temperature—conversion curves for the first decomposition step were modelled with the equations given in Table 2. The results are given in Table 3. The data show that the variances of the models tested are virtually equal for each experiment. Thus, each model results in the same quality of fit. However, the activation energies differ for each model and depend on n . This effect was also found by Dharwadkar et al. [11] and predicted and explained in ref. 8. Only for the correct value of n will the calculated activation energy be identical with the value found from isothermal experiments. The best representation of the isothermal experiments was by the model $[-\ln(1 - \alpha)]^{1/2}$, with $E = 121 \text{ kJ mole}^{-1}$ and $A = 8.9 \times 10^{11} \text{ s}^{-1}$ [3]. When the results obtained in non-isothermal experiments are fitted with the same model, the activation energy at a very low heating rate ($\approx 0.035^\circ\text{C s}^{-1}$) is seen to be close to 121 kJ mole^{-1} , the value found in the previous study; moreover, the pre-exponential factors also agree well. However, the activation energy and pre-exponential factor for higher heating rates are lower (Table 3). Such an effect of the heating rate has been found before [12,13]. In this case it may be due to the presence of water vapour, because Gallagher et al. [14,15] found that water vapour appreciably reduces the activation energy of the decomposition of manganese nitrate. When the heating rate is higher the release of water will be faster and the time available for the water to evaporate and to diffuse out of the sample is less. This results in a higher water vapour concentration, which reduces the activation energy. It would also explain why Gallagher et al. found an activation energy of approximately 90 kJ mole^{-1} for the first decomposition step, whereas from our

TABLE 3

Results obtained in modelling the first decomposition step

Heating rate (°C s ⁻¹)	Model [-ln(1 - α)] ^{1/4}			Model [-ln(1 - α)] ^{1/3}			Model [-ln(1 - α)] ^{1/2}		
	A (s ⁻¹)	E (kJ mole ⁻¹)	Variance	A (s ⁻¹)	E (kJ mole ⁻¹)	Variance	A (s ⁻¹)	E (kJ mole ⁻¹)	Variance
0.034	1.7 × 10 ³	49	9.8 × 10 ⁻⁴	4.4 × 10 ⁵	68	9.7 × 10 ⁻⁴	2.5 × 10 ¹⁰	105	9.6 × 10 ⁻⁴
0.035	1.8 × 10 ⁴	56	1.7 × 10 ⁻³	6.7 × 10 ⁶	76	1.7 × 10 ⁻³	2.3 × 10 ¹²	119	1.6 × 10 ⁻³
0.035	2.1 × 10 ⁴	57	1.7 × 10 ⁻³	1.2 × 10 ⁷	78	1.7 × 10 ⁻³	3.5 × 10 ¹²	121	1.7 × 10 ⁻³
0.035	1.1 × 10 ⁴	56	2.7 × 10 ⁻³	4.9 × 10 ⁶	76	2.7 × 10 ⁻³	7.7 × 10 ¹¹	117	2.7 × 10 ⁻³
0.061	4.4 × 10 ¹	37	1.9 × 10 ⁻³	2.6 × 10 ³	51	1.9 × 10 ⁻³	8.9 × 10 ⁶	79	2.0 × 10 ⁻³
0.066	3.8 × 10 ²	44	4.6 × 10 ⁻⁴	4.8 × 10 ⁴	61	4.6 × 10 ⁻⁴	6.9 × 10 ⁸	94	4.6 × 10 ⁻⁴
0.118	5.7 × 10 ²	44	6.1 × 10 ⁻⁴	6.8 × 10 ⁴	60	6.0 × 10 ⁻⁴	8.9 × 10 ⁸	94	6.0 × 10 ⁻⁴
0.125	3.2 × 10 ²	41	3.4 × 10 ⁻⁴	3.1 × 10 ⁴	56	3.4 × 10 ⁻⁴	2.8 × 10 ⁸	87	3.5 × 10 ⁻⁴
0.185	1.4 × 10 ¹	29	4.2 × 10 ⁻⁴	4.1 × 10 ²	41	4.3 × 10 ⁻⁴	3.7 × 10 ⁵	64	4.4 × 10 ⁻⁴

TABLE 4

Results obtained in modelling the second decomposition step

Heating rate (°C s ⁻¹)	Model [-ln(1 - α)] ^{1/4}			Model [-ln(1 - α)] ^{1/3}			Model 1 - (1 - α) ^{1/3}		
	A (s ⁻¹)	E (kJ mole ⁻¹)	Variance	A (s ⁻¹)	E (kJ mole ⁻¹)	Variance	A (s ⁻¹)	E (kJ mole ⁻¹)	Variance
0.034	3.6 × 10 ¹⁶	172	1.2 × 10 ⁻³	5.5 × 10 ⁹	112	1.1 × 10 ⁻³	1.3 × 10 ¹⁴	155	2.9 × 10 ⁻³
0.035	1.1 × 10 ¹⁶	164	3.2 × 10 ⁻⁴	2.6 × 10 ⁹	107	3.1 × 10 ⁻⁴	3.5 × 10 ¹³	148	8.3 × 10 ⁻⁴
0.035	3.6 × 10 ¹⁴	151	3.7 × 10 ⁻⁴	2.7 × 10 ⁸	98	3.6 × 10 ⁻⁴	2.3 × 10 ¹²	137	1.0 × 10 ⁻³
0.035	1.2 × 10 ¹⁵	157	8.7 × 10 ⁻⁴	5.8 × 10 ⁸	102	8.1 × 10 ⁻⁴	2.8 × 10 ¹²	139	2.1 × 10 ⁻³
0.061	3.5 × 10 ¹³	145	2.8 × 10 ⁻⁴	6.8 × 10 ⁷	94	2.8 × 10 ⁻⁴	1.6 × 10 ¹¹	129	3.8 × 10 ⁻⁴
0.066	1.1 × 10 ¹⁷	177	6.4 × 10 ⁻⁴	1.4 × 10 ¹⁰	115	6.2 × 10 ⁻⁴	2.5 × 10 ¹⁴	159	1.4 × 10 ⁻³
0.118	3.8 × 10 ¹⁶	171	4.3 × 10 ⁻³	5.7 × 10 ⁹	110	3.5 × 10 ⁻³	2.0 × 10 ¹⁴	156	6.7 × 10 ⁻³
0.125	4.3 × 10 ¹⁴	156	6.1 × 10 ⁻³	5.5 × 10 ⁸	103	5.2 × 10 ⁻³	3.4 × 10 ¹²	142	9.5 × 10 ⁻³
0.185	3.4 × 10 ¹⁴	151	7.2 × 10 ⁻³	2.5 × 10 ⁸	96	6.8 × 10 ⁻³	1.8 × 10 ¹²	136	8.5 × 10 ⁻³
Average	2.5 × 10 ^{15*}	160		1.1 × 10 ^{9*}	104		10 ^{13*}	145	

* Calculated from ln A values.

studies approximately 120 kJ mole^{-1} resulted. Gallagher et al. used much larger samples, i.e. about 15 mg, and a lower $\text{Mn}(\text{NO}_3)_2$ concentration. Additional experiments will be carried out to elucidate the effect of water vapour more completely.

The results for the second decomposition step are given in Table 4. No effect of heating rate is found. The variances for the model $[-\ln(1 - \alpha)]^{2/3}$ are lowest; however, this model does not apply because it leads to a mean value for E of $\sim 104 \text{ kJ mole}^{-1}$, i.e. much lower than the average value of 141 kJ mole^{-1} obtained from isothermal experiments. In this respect, the mean value for the model $1 - (1 - \alpha)^{1/3}$ of 145 kJ mole^{-1} is much more satisfactory (Table 1). Thus, despite the higher variances this model is preferred for the second decomposition step because the kinetic parameters for isothermal and non-isothermal experiments should be about equal. The pre-exponential factor (A) averages 10^{13} s^{-1} (calculated from $\ln A$ values) and is only slightly higher than the value observed in isothermal experiments. It is partly compensated by the slightly higher activation energy. Figure 1 shows the fit of the model $1 - (1 - \alpha)^{1/3}$ to a measured temperature—conversion curve. The fit is rather satisfactory.

It is concluded that though a model may give the best fit for non-isothermal experiments it is not necessarily the correct one. It should be checked by performing isothermal experiments and comparison of the results. The type of model used in this work implies that the decomposition proceeds via a surface reaction. However, additional evidence will be needed to confirm this assumption.

Table 5 lists the results obtained in modelling the decomposition of anhydrous manganese nitrate. As was found for the second decomposition step, there is no effect of heating rate. The best fit is usually obtained for the model $[-\ln(1 - \alpha)]^{2/3}$, which also resulted in a good fit for the isothermal experiments. However, the activation energy obtained ($\sim 109 \text{ kJ mole}^{-1}$) is somewhat higher than that obtained from isothermal experiments ($\sim 92 \text{ kJ mole}^{-1}$). Therefore, a few additional models of the form $[-\ln(1 - \alpha)]^{1/n}$ were tried, with $1/n = 0.6, 0.7$ and 0.8 . The results are given in Table 6. The variances for the different models are about equal, thus discrimination between the models is impossible. However, it is again found that E depends on n ; therefore, the model is chosen for which the activation energy corresponds best to the value obtained from isothermal measurements. The activation energy of $\sim 97 \text{ kJ mole}^{-1}$ for $n = 0.6$ corresponds best to the value obtained from isothermal experiments of $\sim 92 \text{ kJ mole}^{-1}$. Figure 2 shows the fit of the model $[-\ln(1 - \alpha)]^{0.6}$ to a measured temperature—conversion curve; again, agreement is satisfactory. The mean value of the pre-exponential factor (A) was calculated from $\ln A$ values and amounts to $8 \times 10^7 \text{ s}^{-1}$. It is slightly higher than the A value obtained from isothermal experiments, but this is compensated by the higher activation energy. Thus the decomposition is described best by the model $[-\ln(1 - \alpha)]^{0.6}$, with an activation energy of 92 kJ mole^{-1} and a pre-exponential factor of $2 \times 10^7 \text{ s}^{-1}$. The values obtained from isothermal experiments are applied because they hardly depend on the type of model (Table 1) and therefore also apply to the model $[-\ln(1 - \alpha)]^{0.6}$.

TABLE 5

Results obtained in modelling the decomposition of anhydrous manganese nitrate

Heating rate (°C s ⁻¹)	Model $[-\ln(1-\alpha)]^{2/3}$			Model $1-(1-\alpha)^{1/3}$		
	A (s ⁻¹)	E (kJ mole ⁻¹)	Variance	A (s ⁻¹)	E (kJ mole ⁻¹)	Variance
0.029	2.4×10^{18}	192	7.8×10^{-4}	7.7×10^{10}	126	6.7×10^{-4}
0.028	4.9×10^{13}	148	5.4×10^{-4}	6.0×10^7	96	4.8×10^{-4}
0.062	1.7×10^{17}	182	4.0×10^{-3}	1.5×10^{10}	118	3.2×10^{-3}
0.060	9.9×10^{14}	160	4.9×10^{-4}	5.8×10^8	104	4.6×10^{-4}
0.162	3.0×10^{14}	158	9.1×10^{-4}	3.5×10^8	102	8.1×10^{-4}
0.159	1.6×10^{15}	166	1.2×10^{-3}	1.1×10^9	108	1.1×10^{-3}
Average	4.6×10^{15} *	168		1.6×10^9 *	109	

* Calculated from ln A values.

TABLE 6

Additional results obtained in modelling the decomposition of anhydrous manganese nitrate

Heating rate (°C s ⁻¹)	Model $[-\ln(1-\alpha)]^{0.6}$			Model $[-\ln(1-\alpha)]^{0.7}$			Model $[-\ln(1-\alpha)]^{0.8}$		
	A (s ⁻¹)	E (kJ mole ⁻¹)	Variance	A (s ⁻¹)	E (kJ mole ⁻¹)	Variance	A (s ⁻¹)	E (kJ mole ⁻¹)	Variance
0.029	2.5×10^9	112	6.5×10^{-4}	4.4×10^{11}	132	6.8×10^{-4}	7.7×10^{13}	152	7.1×10^{-4}
0.028	3.9×10^6	85	4.7×10^{-4}	2.4×10^8	101	4.9×10^{-4}	1.4×10^{10}	116	5.0×10^{-4}
0.062	6.1×10^8	105	3.1×10^{-3}	7.8×10^{10}	124	3.3×10^{-3}	9.9×10^{12}	144	3.5×10^{-3}
0.060	3.2×10^7	93	4.5×10^{-4}	2.4×10^9	110	4.6×10^{-4}	1.8×10^{-4}	126	4.7×10^{-4}
0.162	2.2×10^7	91	7.9×10^{-4}	1.4×10^9	108	8.2×10^{-4}	8.3×10^{10}	124	8.5×10^{-4}
0.159	6.5×10^7	96	1.1×10^{-3}	4.7×10^9	114	1.1×10^{-3}	3.3×10^{11}	131	1.2×10^{-3}
Average	8.1×10^7 *	97		7.1×10^9 *	115		6.1×10^{11} *	132	

* Calculated from ln A values.

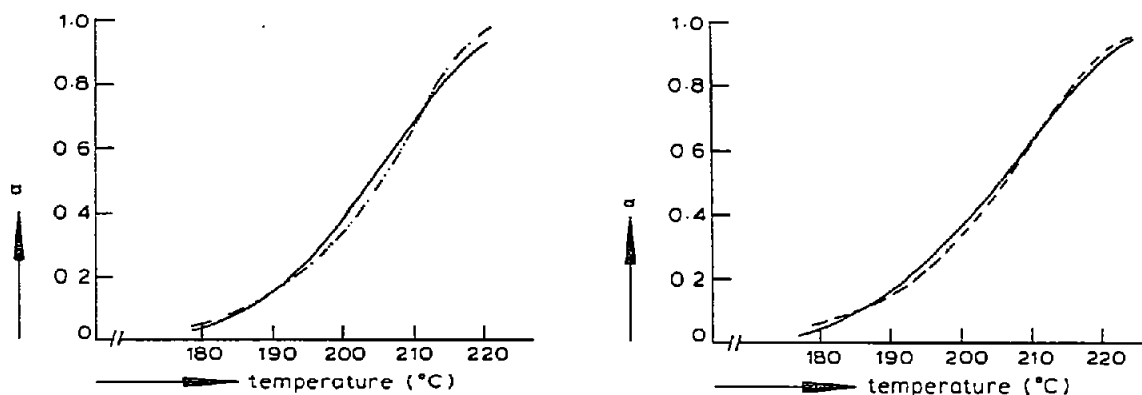


Fig. 1. Measured and calculated temperature—conversion curves for the second decomposition step. (—) Measured curve; (---) $g(\alpha) = 1 - (1 - \alpha)^{1/3}$.

Fig. 2. Measured and calculated temperature—conversion curve for the decomposition of anhydrous manganese nitrate. (—) Measured curve; (- - - -) $g(\alpha) = [-\ln(1 - \alpha)]^{0.6}$.

From the order of the reaction a probable reaction mechanism can be derived. $n = 1.67$ implies that the reaction may proceed by formation of nuclei at a decreasing rate combined with growth into one direction (i.e. rods), because with decreasing nucleation rate the order n is between that of the mechanism with constant and zero nucleation rate, i.e. between 2 and 1 [16].

The results of each decomposition show relatively large variations in pre-exponential factor and activation energy. However, the differences in the reaction rate constant are much smaller: the deviation of the pre-exponential factor and activation energy from their average values largely compensate each other in the reaction rate constant. The often mentioned argument in favour of performing non-isothermal experiments instead of isothermal experiments, namely that only one non-isothermal experiment is needed to establish the kinetic parameters of a reaction, does not seem to be valid, at least not for the reactions investigated. The results from only one specific experiment can deviate appreciably from the correct values (see Tables 4 and 6) and therefore several experiments must be performed to obtain average values.

CONCLUSIONS

The decomposition of aqueous manganese nitrate solutions occurs in two steps. The first step is best described by the model for two-dimensional growth of a constant number of nuclei. The kinetic parameters were found to depend on the heating rate, an effect that may be caused by differences in water vapour concentration.

The second decomposition step is independent of the heating rate and can be described by the model $1 - (1 - \alpha)^{1/3}$, with an activation energy of 145 kJ mole⁻¹ and a pre-exponential factor of 10^{13} s⁻¹. These results agree well

with those obtained from isothermal experiments [3].

Both isothermal and non-isothermal experiments on the decomposition of anhydrous manganese nitrate can be described by the model $[-\ln(1 - \alpha)]^{0.6}$. The activation energy and pre-exponential factor are 92 kJ mole^{-1} and $2 \times 10^7 \text{ s}^{-1}$, respectively. From the order of the reaction it is concluded that the decomposition is probably characterised by a decreasing nucleation rate and one-dimensional growth.

One non-isothermal experiment may not be sufficient to establish kinetic parameters correctly. Owing to the relatively large differences which may occur in the results, several experiments are needed.

REFERENCES

- 1 T.J.W. de Bruijn, W.A. de Jong and P.J. van den Berg, *Thermochim. Acta*, 45 (1981) 265.
- 2 T.J.W. de Bruijn, G.M.J. de Ruiter, W.A. de Jong and P.J. van den Berg, *Thermochim. Acta*, 45 (1981) 279.
- 3 T.J.W. de Bruijn, A.N. Ipekoğlu, W.A. de Jong and P.J. van den Berg, *Thermochim. Acta*, 45 (1981) 293.
- 4 A.B. Zdanovskii and G.É. Zheknina, *Zh. Prikl. Khim. (Leningrad)*, 48 (2) (1975) 427.
- 5 J.M. Criado and J. Morales, *Thermochim. Acta*, 16 (1976) 382.
- 6 J. Sesták, *Proc. 3rd Int. Conf. Therm. Anal.*, Davos, Vol. 2, 1971, p. 3.
- 7 D.W. Henderson, *J. Therm. Anal.*, 15 (1979) 325.
- 8 T.J.W. de Bruijn, W.A. de Jong and P.J. van den Berg, *Thermochim. Acta*, 45 (1981) 315.
- 9 C.D. Doyle, *J. Appl. Polym. Sci.*, 5 (15) (1961) 285.
- 10 A.W. Coats and J.P. Redfern, *Nature (London)*, 201 (1964) 68.
- 11 S.R. Dharwadkar, M.S. Chandrasekharaiah and M.D. Karkhanavala, *Thermochim. Acta*, 25 (1978) 372.
- 12 C.G.R. Nair and K.N. Ninan, *Thermochim. Acta*, 23 (1978) 161.
- 13 K.N. Ninan and C.G.R. Nair, *Thermochim. Acta*, 37 (1980) 161.
- 14 P.K. Gallagher, F. Schrey and B. Prescott, *Thermochim. Acta*, 2 (1971) 405.
- 15 P.K. Gallagher and D.W. Johnson, *Thermochim. Acta*, 2 (1971) 413.
- 16 J. Sesták, V. Satava and W.W. Wendlandt, *Thermochim. Acta*, 7 (1973) 333.